

Andreev Reflection and Long-Range Proximity Effect in Pb/LaCaMnO Point Contacts

V. N. Krivoruchko, V. Yu. Tarenkov, A.I. D'yachenko, and V.N. Varyukhin

Donetsk Physics & Technology Institute NAS of Ukraine,

Str. R. Luxemburg 72, 83114 Donetsk, Ukraine

(Dated: December 21, 2018)

Abstract

The Andreev reflection (AR) spectroscopy has been used to probe mutual influence of superconducting pairing and ferromagnetic correlations in contacts of low-temperature superconductor (S), Pb, and half-metallic ferromagnetic, $\text{La}_{0.65}\text{Ca}_{0.35}\text{MnO}_3$ (LCMO). Two different AR spectra have been observed. In the contacts without proximity effect, the AR spectra reveal a behavior typical for superconductor/spin-polarized metal contacts. In the contacts, which we distinguish as the proximity affected ones, a few unusual effects have been detected. Namely, we have observed: (i) a spectacular drop in the resistance of the contacts at the onset of the Pb superconductivity; (ii) a typical for S/normal nonmagnetic metal contacts, excess current and doubling of the normal-state conductance; and (iii) a much larger than it should be for conventional superconductivity ratio of the single-particle gap to the Pb superconducting transition temperature. The very distinct AR characteristics of proximity affected contacts observed by us suggest unconventional (triplet) superconducting pairing and long-range proximity effect at S/LCMO interface.

Introduction. - Electron transport in ferromagnetic (F) metal/superconductor (S) heterocontacts has attracted considerable attention recently. The key phenomenon that controls the behavior of such systems is proximity effect [1-3]. Theory predicts that in the extreme case of a completely spin-polarized material the conventional (singlet s-wave pairing) proximity effect is absent [4]. Therefore one might expect that the influence of the superconducting proximity effect on the transport properties of such heterostructures should be negligibly small. A rapidly growing number of experiments seem, however, to contradict these conclusions and show that a novel type of proximity effect may be realized in S/F proximity coupled structures. Kasai *et al.* [5] were the first to our knowledge who asserted this hypothesis based on the results of the investigation of current-voltage characteristics for $\text{YBa}_2\text{Cu}_3\text{O}_y$ /magnetic manganese oxide/ $\text{YBa}_2\text{Cu}_3\text{O}_y$ junctions. For certain values of x , the authors observed that supercurrent passes through a half-metallic ferromagnetic (HMF) layers up to 200nm thickness. These results can not be explained in paradigms of the conventional proximity effect and suggested a novel long-range proximity effect concerned with magnetism of the barrier. An unconventional mutual influence of superconductors and ferromagnetic conductors in hybrid S/F nanostructures was also reported recently by a few groups [6-11].

Despite the existing experimental evidences supporting unconventional proximity effect in S/HMF structures, understanding of this phenomenon still remains unclear and requires direct measurement of such intrinsic characteristics of the superconducting state as the local quasiparticle density of states (DOS), value of the superconducting gap, spin symmetry of the pairs, etc. As is well known, such methods as tunnelling spectroscopy [12] and Andreev reflection (AR) spectroscopy [13] are direct and sensitive tools for these purposes. In particular, recently the crossed AR spectroscopy of a metallic point contact has been discussed as a sensitive probe of superconducting order parameter spin-symmetry [14,15].

In this report, first to our best knowledge, the AR spectroscopy has been utilized to probe the unconventional superconducting pairing in contacts of low-temperature superconductor and a half-metallic ferromagnet. If triplet pairing exists in S/HMF heterostructures, the S/F point contacts should reveal such typical for S/normal nonmagnetic metal (N) contacts distinct features as excess current and doubling of the normal-state conductance, which have not yet been demonstrated in experiment until now. Such material as Pb is used as the superconducting electrode and $\text{La}_{0.65}\text{Ca}_{0.35}\text{MnO}_3$ (LCMO) as the HMF. Two qualitatively

different AR spectra have been detected. In the contacts without visible proximity effect, the AR spectra reveal a behavior typical for S/spin polarized metal contacts (see, e.g., Refs. [16-19]). In the contacts with visible superconducting proximity effect, new phenomena have been observed. Namely, a typical for S/N interface, excess current and considerable increase (doubling) of the contact's conductance below the superconducting critical temperature have been detected. Restored magnitude of the single quasiparticle gap is anomalously larger than one can expect for conventional BCS model $\Delta_{BCS}(T=0)/T_C$ ratio. Incorporating the inherent magnetic nonhomogeneity of manganites, we speculate possible physical mechanisms behind the observed unconventional features of the AR spectra. Our results provide spectroscopic evidence for existence of triplet superconducting pairing and long-range proximity effect at S/HMF boundary.

Experimental details. – We have studied point contacts with geometry shown in Fig. 1. Textured LCMO plates were grown using standard ceramic technique. In particular, ceramic powder plates sized $0.1 \times 1 \times 10 \text{ mm}^3$ were pressed (20 Kbar) and then subjected to annealing for 8h at 1250°C . This leads to an increase of the average size values of crystallites up to values about 5-10 μm . The resistivity was measured by the standard four-probe method with the low frequency ac technique. A typical low-temperature superconductor Pb has been used as a superconducting electrode. Metallic contacts between LCMO plate and superconducting wire were formed by pressing slide-squash up a needle-shaped Pb against the LCMO surface. The contacts were made at room temperature and at liquid nitrogen, as well, but the results did not depend upon the way of preparation. The contacts' parameters were stable, offering a possibility to perform measurements in wide temperature range. Note, that in comparison to manganites/high- T_C S structures in our Pb/LCMO contacts the so-called hole-charge transfer effect [20] is not present.

Temperature dependence of the plates' resistance (see bottom insert in Fig. 2) has a sharp maximum near $T_{Curie} \approx 270\text{K}$ associated with the well known metal-dielectric transition [21]. Below room-temperature the resistance of the plates was $\sim 1\Omega$. The low-field ($H \approx 100 \text{ Oe}$) magnetoresistive effect $[\rho(T,0) - \rho(T,H)]/\rho(T,0)$ at $T = 77\text{K}$ was only 0.3% (not shown). This suggests that the contribution of inter granular junctions to the total sample resistance is negligibly small. The transition resistance of the current and potential contacts was $R \sim 10^{-8} \Omega \times \text{cm}^2$. The junctions resistance was much larger ($\sim 100 \Omega$), so that the rescaling effects can be neglected.

The approximate value of the contact diameter d is estimated by employing the Wexler's formula [22]. We obtain $d \sim 100\text{\AA}$, that is we deal with the so-called Sharvin contacts [23]. Taking into account small contact's dimension we estimate the specific resistivity of the micro crystals is of the order $\rho \sim 10^{-4}\Omega \times \text{cm}$, and for the mean free path we obtain $l \sim 100\text{\AA}$. Since the mean free path l is an order of the contact diameter d , this means that the transport regime is into the intermediate region, etc., not a ballistic ($l \gg d$), and not a diffusive one ($l \ll d$). (Experimental details can be found in Ref. 24).

Results. – We recorded about a hundred of the AR spectra. Mostly, we observed the well known spectrum that reflects the half-metallic properties of LCMO. Representative normalized differential conductance $G(V) = (dI/dV)(V/I)$ of the Pb/LCMO junction is shown in Fig. 3. As one can see, in contrast to the conventional AR at S/N interface characterized by excess current, here an excess voltage V_{exc} is observed. The almost constant V_{exc} value is observed for $|V| \leq 20\text{mV}$. This proves the suggestion that heating effects could be neglected. Any visible features of superconducting proximity effect have not been detected, and we will refer to these contacts as “the contacts without proximity effect”. For singlet pairing, superconducting coherence length $\xi_F = (\hbar D_F / k_B \pi T_{Curie})^{1/2}$ (in the dirty limit [1-3]) for LCMO is extremely short $\sim 5 \div 7\text{\AA}$ (here D_F denotes the diffusion constant in F). Contribution of such a small region to the contact's resistance is less than 1%.

The suppression of the AR in S/F point contacts has been observed experimentally by several groups [16-19]. These results are qualitatively well explained by de Jong and Beenakker's theory [4]. Using the data in Fig. 3, one can quantitatively restore the degree of the current spin-polarization P_C for LCMO. We analyzed the results obtained on such type contacts on the basis of the ballistic and diffusion models [17,25,26]. The restored magnitude of P_C was 75-85%. (Details will be presented elsewhere, Ref. 24).

For some of cases the measured contact's spectrum reveals very distinct features which we interpret as the manifestation of an unconventional proximity effect. The finger-print of such junctions is a quite visible drop of the contact's resistivity just after superconducting transition of Pb. Pronounced picture of proximity effect we observed on a few junctions. Figure 2 (main panel) shows an example of temperature dependence of the resistance of the proximity affected contact. At $T < 7.2\text{K}$ a sharp drop of the contact's resistivity is observed. Reduction of the resistance δR (about 15%) is by two orders of magnitude larger than it might be expected from the conventional theory of proximity effect for S/F contacts. In

Fig. 4 both the current-voltage and the conductance $G(V) = (dI/dV)/(I/V)$ versus voltage dependences for the Pb/LCMO proximity affected point contact at 4.2K are presented. It is evident that, like for a conventional AR at S/N interface and opposite to the results in Fig. 3, the excess current and doubling of the normal-state conductivity has been observed.

For S/N structure, the AR acts as a parallel conduction channel to the initial electron current, doubling the normal-state conductance G_N of the point contact for applied voltage $eV < \Delta_1$, where Δ_1 is the single-particle gap at the interface. As it follows from the experimental results in Fig. 4, the proximity induced single-particle gap at Pb/LCMO interface, $\Delta_1 \approx 18$ meV, is much larger than that of Pb: $\Delta_{Pb}(T = 0) = 1.41$ meV. In Fig. 5 the temperature dependence of the AR spectra for another proximity affected Pb/LaCaMnO contact is shown. As it is seen, the supercurrent conversion into quasiparticle current by AR mechanism takes place up to 7.04K, while the ratio $G(0)/G(eV > \Delta)$ is notably decreased. This proves that the superconductivity of LCMO is due to superconducting state of Pb. Fondly comparing the value of proximity induced single-particle gap $\Delta_1 \approx 18$ meV and T_C ($= 7.2$ K for bulk Pb), one can find that for proximity induced superconducting state of S/LCMO interface the conventional BCS ratio $\Delta_{BCS}(T = 0) = 1.76T_C$ does not hold.

We should note that for some contacts we detected the AR spectrum that may be considered as evidence of coexistence at S/LCMO interface of both conventional and unconventional superconducting pairing. Representative data for such contacts is shown in Fig. 6. Also, in Figs. 4 and 5 for voltage $eV > \Delta_1$, one can distinguish the peaks which we attributed are due to a formation of the so-called “phase-slip lines” – the two-dimensional analogue of phase-slip centers [27,28]. Directly the existence of phase slipping is visible in Fig. 7, where representative excess current-voltage (I_{exc} -V) dependence is shown. There we observe several features which are characteristic to phase-slip lines [27,28]: (i) a voltage jump at some critical current; (ii) all resistive branches have the same excess current, given by the intersection of their slopes with current axis. The value of the excess current is found to fulfill the theoretical relation $I_{exc} = (4/3)\Delta_1/eR_N$ [29] for $\Delta_1 \approx 18$ meV and experimental value of the contact’s normal state resistance $R_N = 232 \Omega$. I.e., the excess current can not be attributed to Pb electrode. The step-like increasing of the contact’s resistance is due to a discrete destruction (phase-slip) of superconducting state of surface region LCMO. One can make a crude estimation about the thickness of this surface region, L_{SC} , being in superconducting state. Indeed, the thickness of the normal-state layer for each phase-slip line

is of the order $2\xi_{LCMO}$, where ξ_{LCMO} is the superconducting coherence length of LCMO, $\xi_{LCMO} \approx \hbar v_F / \Delta_{LCMO}$. For manganites the Fermi velocity v_F is $\sim 10^7$ sm/sec and taking naively (see Discussion) $\Delta_{LCMO} \sim \Delta_1$ one can easily obtain $\xi_{LCMO} \approx 30 \text{ \AA}$. In Fig. 7, six jumps are definitely detected. I.e., L_{SC} is about $6(2\xi_{LCMO}) \sim 300\text{-}400 \text{ \AA}$. If we assume that Δ_{LCMO} is about Δ_{Pb} , then the thickness of the surface region with proximity induced superconductivity is larger by order.

Discussions. – The exact processes of conversion by which the supercurrent is continued as the quasiparticle current in an adjacent half-metal ferromagnetic layer are not known yet. Recent theories proposed a few mechanisms which may cause a nonvanishing Josephson and long-range proximity effects in S/HMF/S structures. The most elaborated one is based on the induced triplet correlations which result in the indirect proximity effect. In the model [30,31] the presence of the superconducting triplet correlations with an unusually long penetration length in the ferromagnetic metal requires the interplay of two separate interface processes: spin mixing and spin-flip scattering. The spin-rotation effect alone generates at the superconducting side of the S/HMF boundary the triplet correlation with “zero spin” component of the form $f_{\uparrow\downarrow} + f_{\downarrow\uparrow}$ (here $f_{\uparrow\downarrow}$ and $f_{\downarrow\uparrow}$ stand for opposite-spin triplet pair amplitudes). Similar to a wave function of the singlet (Cooper) pair, this component penetrates into HMF on a short distance $\xi_F \sim (\hbar D_F / \pi H_{exc})^{1/2} \sim (\hbar D_F / \pi k_B T_{Curie})^{1/2} \ll \xi_S$ (here H_{exc} denotes the exchange energy). Spin-flip scattering induces both “nonzero spin” triplet components of the pair amplitudes, $f_{\uparrow\uparrow}$ and $f_{\downarrow\downarrow}$, in the superconductor, and the $f_{\uparrow\uparrow}$ (or $f_{\downarrow\downarrow}$) pair amplitude in the half metal ferromagnet. The equal-spin triplet correlations $f_{\uparrow\uparrow}$ and $f_{\downarrow\downarrow}$ possess an unusually long penetration length in the ferromagnet, such as for normal nonmagnetic metal: $\xi \sim (\hbar D_F / \pi k_B T)^{1/2} \sim \xi_N$. The long-range triplet correlations may also arise in S/F structures with a nonuniform magnetization in the ferromagnet [32-34]. Remarkably, the local magnetic nonhomogeneity of S/F interface, no matter whether it has been introduced as a “spin-active” interface or as a nonuniform magnetization, is a key factor of the models [30-34]. At present, however, no existing technology can create such nonhomogeneity in a controllable way with nanoscale precision.

On the other hand, several theoretical models and numerous experimental data suggest that nano-scale nonhomogeneity, referred to as phase separation, is an intrinsic feature of colossal magnetoresistive manganites (see for example Ref. [21] and references therein). In particular, the following draft picture for a surface (thickness of a few nanometers) magnetic

structure of manganites has emerged at present: since the double exchange mechanism is sensitive to a Mn-O-Mn bound state, any structural disorder (oxygen non-stoichiometry, vacancies, stress, etc.) near surface region of grain suppresses the double exchange and leads to a local spin disorder. In particular, for $\text{La}_{1-x}\text{Ca}_x\text{MnO}_3$ with $x \approx 0.3$, scanning tunneling spectroscopy [35] and neutron diffuse scattering [36] indicate the existence of magnetic nonhomogeneities attributed to hole-rich and hole-poor clusters and even allow to estimate the shape and the size (a few lattice spacings) as well as the magnetic structure of the clusters. Another feature important for our discussion is that, due to strong Hund's interaction (for Mn^{3+} the Hund's energy $\sim 1\text{eV}$ [21]), spin disorder serves as strong spin-scattering centers for charge carries.

Incorporating the internal magnetic nonhomogeneity of LCMO, the AR spectra observations can be explained as follows. For the Sharvin contacts “without proximity effect”, the large but not full spin polarization of transport in LCMO most naturally can be explained in the model of magnetic phase segregation of the crystal on a nanometer scale where only one phase corresponds to the state of the ferromagnetic metal with full charge carriers spin polarization. (The details of such physics behind the observed incomplete spin polarization of transport in manganites are discussed in Ref. [24].) For “proximity affected contacts”, the observed large change in the contact's resistance together with its sing can not be explained on the basis of conventional, i.e., singlet pairing, superconducting proximity effect. We supposed that in such contacts the conditions for unconventional proximity effect are fulfilled. I.e., depending on the exact magnetic nonhomogeneity at S/HMF boundary, the LCMO surface causes superconducting triplet $f_{\uparrow\uparrow}$ (or $f_{\downarrow\downarrow}$) correlations which decay slowly into the half-metal. Being proximity induced, the supercurrent of equal-spin triplet pairs is continued as a quasiparticle current in a bulk of the half-metal ferromagnetic layer through a usual Andreev reflection mechanism, with an excess current and doubling of the normal-state conductance for applied voltage less than the single-particle gap.

At this stage we can only speculate about the discrepancy between the proximity induced single-particle gap at Pb/LCMO interface and the superconducting gap of Pb. The value of the single-particle gap Δ_1 obtained from the AR spectra may be qualitatively justified by generating the models of superconductivity of strongly disordered (granular) superconductors [37,38] on our case of proximity induced triplet superconductivity of phase-separated manganites. It has been known for many years (see, e.g., [39]) that some superconductors,

when composed of small grains, show the Δ/T_C ratio higher than the BCS value. Intuitively, it is clear that the proximity induced superconducting state of a manganite with hole-rich and hole-poor clusters of a few lattice spacing is practically the same as that of a strongly disordered metal (or metal nanoparticles) with attractive interaction and superconductivity due to a tender coherence between localized Cooper pairs. The strength of disorder can be characterized by two relevant energy scales: δ and Δ_1 , where δ is the effective level spacing in the localization volume, and Δ_1 is the single-particle gap. In the regime $\delta \ll \Delta_{Pb} \ll \Delta_1$ superconductivity persists due to induced triplet pairs. However, due to an extra cost of creating an unpaired electron, the energy required to add an electron in this regime is no longer equal to self-consistent BCS gap and the ratio of this gap to T_C can be anomalously large [38]. I.e, in such system, the superconducting pairing energy does not characterize the spectral gap and the typical single-particle gap Δ_1 , that most naturally is measured by tunnelling or AR spectroscopy experiments, is much larger than T_C .

Conclusion. – In summary, to study superconducting pairing in heterostructures of low-temperature superconductor and a half-metallic ferromagnet, we have prepared the point contacts of Pb/La_{0.65}Ca_{0.35}MnO₃ where the Andreev reflection plays an important role. Several evidence of the existence of unconventional superconducting pairing and long-range proximity effect are detected. In particular, since the supercurrent of equal-spin pairs can be continued as quasiparticle current in a bulk of a half-metal ferromagnet due to usual AR mechanism, such finger-print of AR as excess current and doubling of the normal-state conductance have been observed. The obtained experimental data can be understood within a model of inherent magnetic nonhomogeneity of manganites if one includes concepts (i) of proximity induced superconducting triplet correlations at S/HMF interface with a long-range decay length, and (ii) superconductivity of a phase separated (hole-rich and hole-pore clusters) surface of manganite due to a fragile coherence between localized triplet pairs. It appears that under-doped manganites as well as region at surface of metallic ferromagnetic manganites are convenient materials to reveal new mechanisms of superconductivity. The results obtained are of great relevance for spin-electronics devices based on exploration of the nanoscale magnetism of manganites and their half-metallic features.

Authors acknowledge the participants of the ICFM-05 (Partenit, Crimea, Ukraine) for valuable discussion.

-
1. A. A. Golubov, M. Y. Kupriyanov, and E. Il'ichev, *Rev. Mod. Phys.* **76**, 411 (2004).
 2. A. Buzdin, *Rev. Mod. Phys.* **77**, 935 (2005).
 3. F. S. Bergeret, A. F. Volkov, and K. B. Efetov, *Rev. Mod. Phys.* **77**, #4 (2005).
 4. M. J. M. de Jong and C. W. J. Beenakker, *Phys. Rev. Lett.* **74**, 1657 (1995).
 5. M. Kasai, Y. Kanke, T. Ohno, and Y. Kozono, *J. Appl. Phys.* **72**, 5344 (1992).
 6. V. T. Petrashov, N. V. Antonov, S. Maksimov, and R. Shaikhaidarov, *JETP Lett.* **59**, 551(1994).
 7. V. T. Petrashov, I. A. Sosnin, I. Cox, A. Parsons, and C. Troadec. *Phys. Rev. Lett.* **83**, 3281 (1999).
 8. Z. Sefrioui, D. Arias, V. Peña, J. E. Villagas, M. Varela, P. Prieto, C. Leon, J. L. Martinez, and J. Santamaria, *Phys. Rev. B* **67**, 214511 (2003).
 9. V. Peña, Z. Sefrioui, D. Arias, C. Leon, J. Santamaria, M. Varela, S.J. Pennycook, and J. L. Martinez, *Phys. Rev. B* **69**, 224502 (2004).
 10. K. Senapati and R. C. Budhani, *cond-mat/0507073* (2005).
 11. I. Sonin, H. Cho, V. T. Petrashov, and A. F. Volkov, *cond-mat/0511077* (2005).
 12. E. L. Wolf, *Principles of Electron Tunneling Spectroscopy* (Oxford University Press, New York, 1985).
 13. A. F. Andreev, *Sov. Phys. JETP*, **19**, 1228 (1964).
 14. J. M. Byers and M. E. Flatte, *Phys. Rev. Lett.* **74**, 306 (1995).
 15. D. Beckmann and H. B. Weber, *Phys. Rev. Lett.* **93**, 197003 (2004).
 16. R. J. Soulen Jr., J. M. Byers, M. S. Osofsky, B. Nadgorny, T. Ambrose, S. F. Cheng, P. R. Broussard, C. T. Tanaka, J. Nowak, J. S. Moodera, A. Barry, and J. M. D. Coey, *Science* **282**, 85 (1998).
 17. B. Nadgorny, I. I. Mazin, M. Osofsky, R. J. Soulen, Jr., P. Broussard, R. M. Stroud, D. J. Singh, V. G. Harris, A. Arsenov, and Ya. Mukovskii, *Phys. Rev. B* **63**, 184433 (2001).
 18. Y. Ji, G. J. Strijkers, F. Y. Yang, C. L. Chien, J. M. Byers, A. Anguelouch, G. Xiao, and A. Gupta, *Phys. Rev. Lett.* **86**, 5585 (2001).
 19. G. J. Strijkers, Y. Ji, F. Y. Yang, C. L. Chien, and J. M. Byers, *Phys. Rev. B* **63**, 104510 (2001).

20. A. Hoffmann, S. G. E. Te Velthuis, Z. Sefrioui, J. Santamaria, M. R. Fitzsimmons, S. Park, and M. Varela, *Phys. Rev. B* **72**, 140407 (2005).
21. E. Dagotto, T. Hotta, and A. Moreo, *Phys. Rep.* **344**, 1 (2001).
22. G. Wexler, *Proc. Phys. Soc. London* **89**, 927 (1966).
23. Yu. V. Sharvin, *JETP* **21**, 655 (1965).
24. A.I. D'yachenko, V.A. D'yachenko, V. Yu. Tarenkov, and V. N. Krivoruchko, *Fiz. Tverd. Tela* **48**, #3 (2006).
25. I. I. Mazin, A. A. Golubov, and B. Nadgorny. *J. Appl. Phys.* **89**, 7576 (2001).
26. B. P. Vodopyanov, and L. R. Tagirov, *JETP Lett.* **77**, 126 (2003).
27. I. M. Dmitrenko, *Low. Temp. Phys.* **22**, 686 (2001).
28. A. G. Sivakov, A. M. Glukhov, A. N. Omelyanchouk, Y. Koval, P. Müller, and A. V. Ustinov, *Phys. Rev. Lett.* **91**, 267001 (2003).
29. G. E. Blonder, M. Tinkham, and T. M. Klapwijk, *Phys. Rev. B* **25**, 4515 (1982).
30. M. Eschring, J. Kopu, J. C. Cuevas, and G. Schön, *Phys. Rev. Lett.* **90**, 137003 (2003).
31. T. Champel and M. Eschrig, *B* **72**, 064523 (2005).
32. F. S. Bergeret, A.F. Volkov, and K. B. Efetov, *Phys. Rev. Lett.* **86**, 4096 (2001); *Phys. Rev. B* **64**, 134506 (2001).
33. A. Kadigrobov, R. I. Skekhter, and M. Jonson, *Europhys. Lett.* **54**, 394 (2001).
34. A. F. Volkov, Ya. V. Fominov, and K. B. Efetov, *Phys. Rev. B* **72**, 184504 (2005).
35. M. Fäth, S. Freisem, A. A. Mewnovsky, Y. Tomioka, J. Aarts, and J. A. Mydosh, *Science* **285**, 1540 (1999).
36. M. Hennion, F. Moussa, P. Lehouelleur, F. Wang, A. Ivanov, Y. M. Mukovskii, and D. Shulyatev, *Phys. Rev. Lett.* **94**, 057006 (2005).
37. V. F. Gantmakher, *Physics-Uspekhi* **41**, 214 (1998).
38. M. Feigel'man, L. B. Ioffe and E. A. Yuzbashyan, *cond-mat/0504766* (2005).
39. R. W. Cohen and B. Abeles, *Phys. Rev.* **168**, 444 (1968).

Figure Captures

FIG. 1. Geometry of point contacts under consideration. Proximity affected regions, and magnetic inhomogeneity (hole-rich and hole-pore clusters) of the manganite surface are shown schematically.

FIG. 2. Temperature dependence of the resistance of the proximity affected contact. Upper insert: temperature dependence of the resistance of the proximity affected contact in the region of Lead superconducting transition. Bottom insert: temperature dependence of the LCMO plates' resistance.

FIG. 3. Current-voltage and normalized differential conductance $G(V) = (dI/dV)(V/I)$ of the Pb/LCMO contact without visible superconducting proximity effect; $T = 4.2$ K.

FIG. 4. Current-voltage and normalized conductance $G(V) = (dI/dV)/(I/V)$ vs voltage dependences for proximity affected Pb/LCMO point contact at 4.2K

FIG. 5. Temperature dependence of the AR spectra for proximity affected Pb/LaCaMnO contact. The curves are shifted for clearness.

FIG. 6. An example of complex AR spectra has been observed for some Pb/LCMO contacts.

FIG. 7. The excess current-voltage (I_{exc} -V) characteristic for proximity affected contact. Each voltage jump in I_{exc} -V curve corresponds to a generation of an additional phase-slip line in the surface region of LCMO.

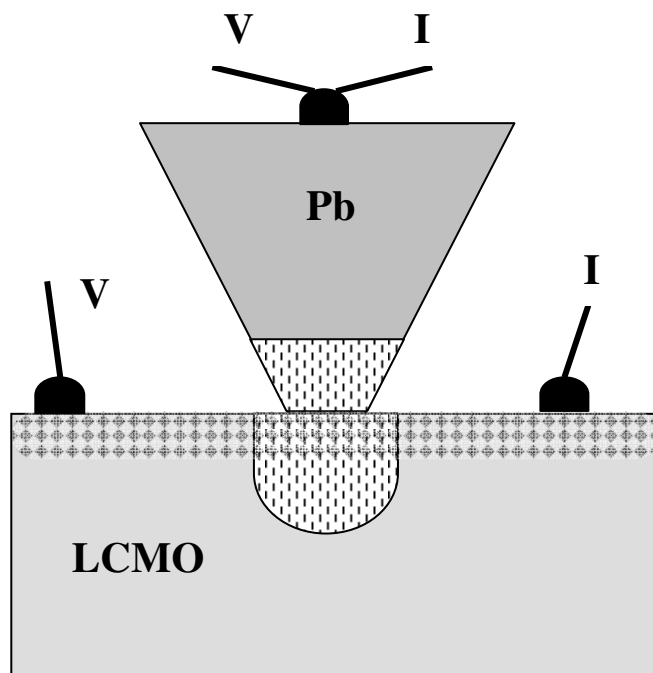


Fig. 1. Krivoruchko

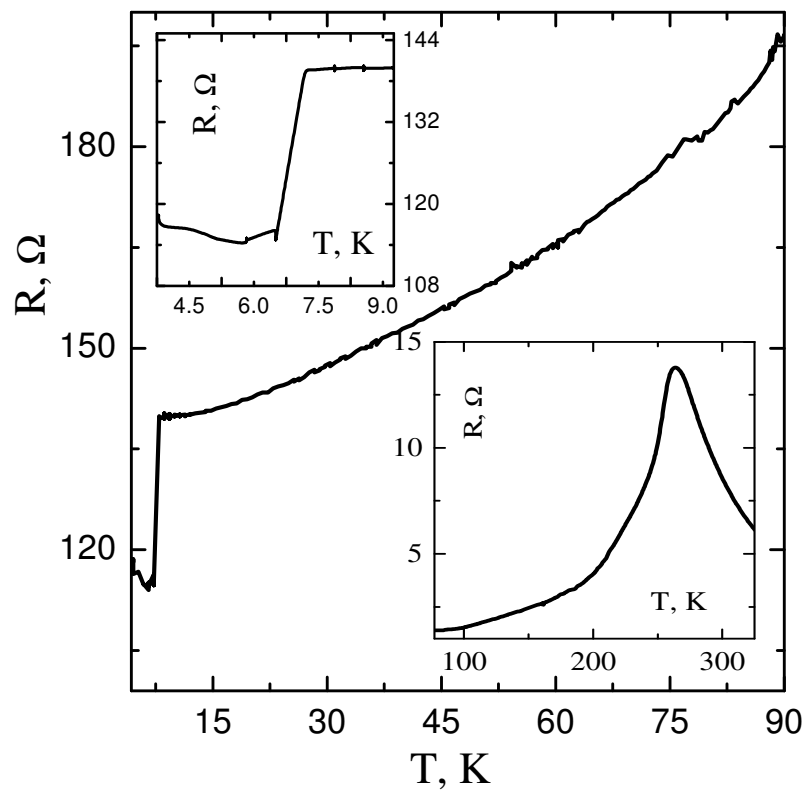


Fig. 2. Krivoruchko

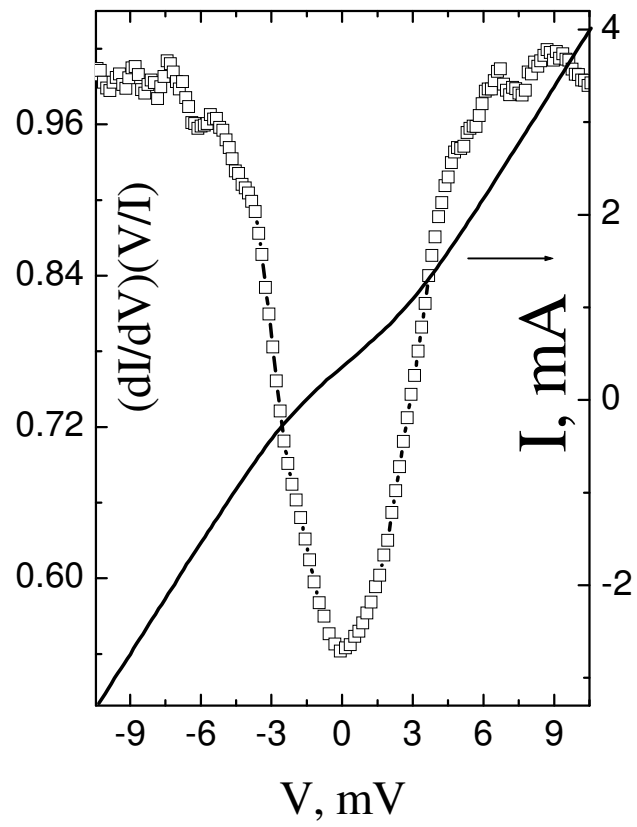


Fig. 3. Krivoruchko

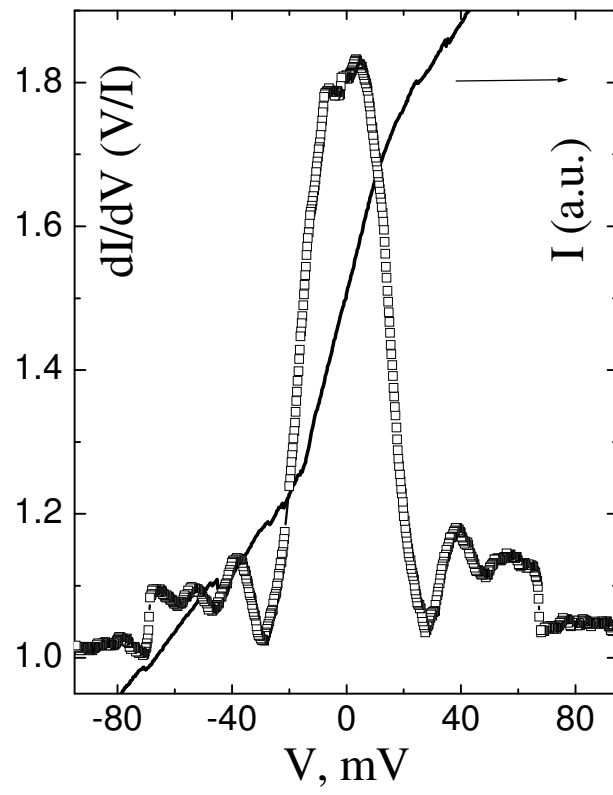


Fig.4. Krivoruchko

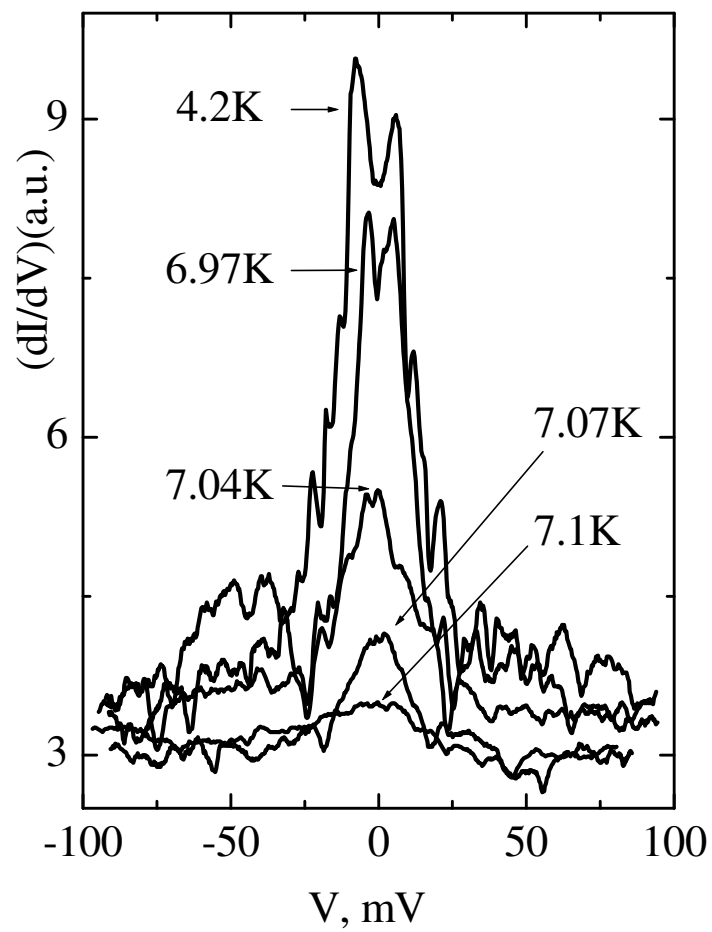


Fig. 5. Krivoruchko

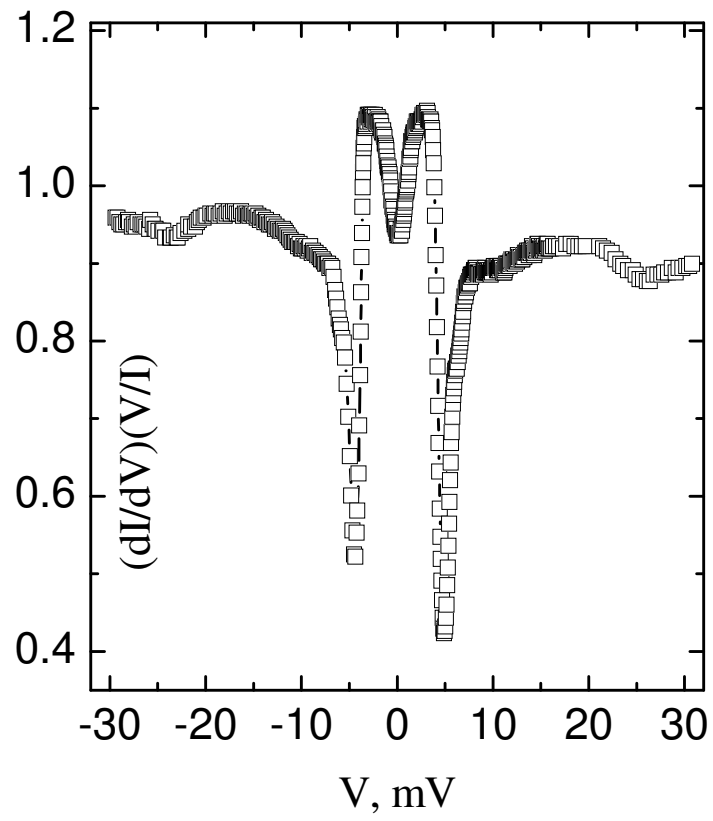


Fig. 6. Krivoruchko

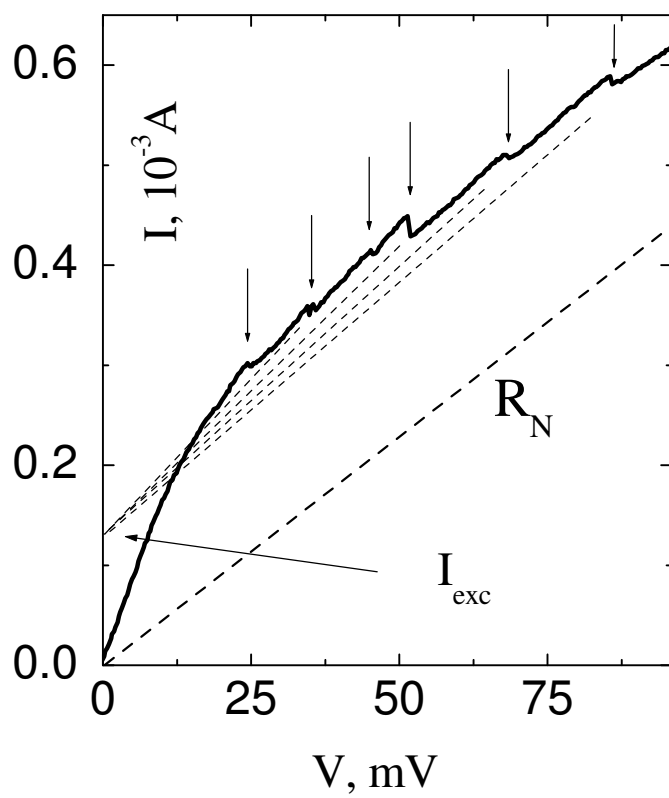


Fig. 7. Krivoruchko